Effects of Ryanoids on Spontaneous and Depolarization-Evoked Calcium Release Events in Frog Muscle

Chiu Shuen Hui,* Henry R. Besch Jr.,† and Keshore R. Bidasee‡
*Department of Cellular and Integrative Physiology and †Department of Pharmacology and Toxicology, Indiana University Medical Center, Indianapolis, Indiana 46202; and ‡Department of Pharmacology, University of Nebraska Medical Center, Omaha, Nebraska 68198

ABSTRACT The effects of ryanoids on calcium sparks and transients were studied in voltage-clamped cut frog muscle fibers with a laser scanning confocal microscope. For each ryanoid employed, several sequential effects were observed, including: a), transient increases in spontaneous spark frequency; b), conversions of sparks to long-lasting steady glows; and c), occasional interruptions of the glows. The ratio of the amplitude of the glow induced by a ryanoid to that of the precursory spark followed the order: ryanodol > ryanodine > C_{10}-O_{eq}-glycyl-ryanodine > C_{10}-O_{eq}-β-alanyl-ryanodol. This sequence of glow amplitudes parallels that of the subconductances induced by these ryanoids in single-channel studies, suggesting that the glows reflect Ca^{2+} fluxes through semiopen calcium release channels. Ryanoids also abolished depolarization-evoked sparks elicited with small pulses, and transformed the calcium release during depolarization to a uniform nonsparking fluorescence signal. The ratio of this signal, averaged spatially, to that of the control followed the order: ryanodol < ryanodine < C_{10}-O_{eq}-glycyl-ryanodine < C_{10}-O_{eq}-β-alanyl-ryanodol, implying an inverse relationship with the amplitudes of ryanoid-induced glows. The observation that depolarization-evoked calcium release can occur after ryanoid suppression of calcium sparks suggests the possibility of a new strategic approach for treating skeletal muscle diseases resulting from leaky calcium release channels.

INTRODUCTION

Release of Ca^{2+} from the sarcoplasmic reticulum (SR) is an essential step in the cascade of events leading to striated muscle contraction. In live cells, the global elevation in myoplasmic Ca^{2+} concentration is believed to arise from the spatial and temporal summation of many localized calcium release events, called calcium sparks. These ''elementary'' events were first detected in cardiac muscle (beginning with Cheng et al., 1993; Lopez-Lopez et al., 1994) and later in skeletal muscle (beginning with Tsugorka et al., 1995; Klein et al., 1996), with the help of laser scanning confocal microscopes. When cells are at rest, calcium sparks occur spontaneously but only infrequently. Upon depolarization, the frequency of calcium sparks increases significantly. These spontaneous and evoked events reflect Ca^{2+} fluxes through a calcium release unit (CRU) consisting of a single, or a few, calcium release channel (CRC).

The plant alkaloid ryanodine (Ry) is a potent and specific modulator of CRCs. Up to low micromolar concentrations, it activates the channels, whereas at higher concentrations, it inhibits the channels. From here on, the ryanoid-induced inhibited state of the channel will be referred to as the ''shut'' state, as previously introduced by Bidasee and Besch (1998), to distinguish it from the resting closed state. Because of the high specificity of Ry binding, CRCs are also called ryanodine receptors (RyRs). The actions of Ry on single RyR have been studied extensively in bilayer preparations, but most of the molecular processes have not been delineated in more physiological preparations. In our recent publication (Hui et al., 2001), we showed that the first of the multiple effects of Ry in cut skeletal muscle fibers was an increase in the frequency of calcium sparks. A similar finding was also reported by Gonzalez et al. (2000). This effect likely results from an increase in open probability, P_0, of the CRCs in a CRU. Single-channel studies suggest that the enhanced P_0 at a low [Ry] results from an increased channel gating frequency (Bull et al., 1989; Buck et al., 1992; Bidasee et al., 2003). Second, some calcium sparks were converted to steady glows that lasted up to many minutes. The glows resembled that observed by Cheng et al. (1993) in the cardiac preparation and likely result from the induction of CRCs to a semiopen state, although this explanation has not been fully established. Third, the glows were interrupted by occasional gaps (short periods of darkness). These gaps probably correspond to the brief transitions of CRCs from the semiopen state to the shut state. Because glows never reverted to sparks, spontaneous transitions of CRCs from the semiopen state to the full open state may be forbidden, at least for Ry per se. With a high [Ry], there was no sign of any calcium release. This corresponds to the long-lasting transition of CRCs to the shut state.

An interesting question that arose from our preceding article (Hui et al., 2001) was whether the gates of the CRCs are ''locked'' rigidly in a semiopen conformation when Ry induces a steady glow. In the presence of an activating (low μM) [Ry], skeletal muscle undergoes an irreversible contracture (Jenden and Fairhurst, 1969). If the contracture is caused by an incessant Ca^{2+} flux through semiopen CRCs, it would imply that persistent closure is unlikely unless

Submitted September 2, 2003, and accepted for publication March 18, 2004.
Address reprint requests to Dr. Chiu Shuen Hui, Dept. of Cellular and Integrative Physiology, Indiana University Medical Center, 635 Barnhill Dr., Indianapolis, IN 46202. Tel.: 317-274-8238; Fax: 317-274-3318; E-mail: cshui@iupui.edu.

0006-3495/04/07/243/13 $2.00
doi: 10.1529/biophysj.103.031435

a higher [Ry] is applied. Such an inability of the channels to open further spontaneously and to close would suggest that the gates may indeed be stuck in the semiopen position, rendering them unresponsive to further activation by depolarization. However, to our surprise, after all calcium sparking activity in a fiber had been abolished by a low [Ry], depolarization did elicit additional calcium release, not in the form of sparks but as a uniform, global increase in fluorescence. Three possibilities were offered in that article to explain the uniform release: a), Although a CRC in the semiopen state cannot open spontaneously to generate sparks, it can be pulled to open further by a voltage sensor, but this triggered opening has altered kinetics so that no spark can be generated. If this is true, the gate of the CRC is not held rigidly in the semiopen position. b), There are two populations of voltage-gated CRCs, one more sensitive to Ry and capable of generating calcium sparks and the other less sensitive to Ry and incapable of generating calcium sparks but capable of generating unresolvable events such as calcium quarks (Lipp and Niggli, 1996). A low [Ry] can shut the former population but not the latter. It may take $\sim$20 μM Ry to completely shut the latter. c), There is only one population of CRCs, but some are linked to dihydropyridine receptors (DHPRs) whereas some are not. After Ry binding, an unlinked CRC is free to make transition to the semiopen state to generate a glow but a linked one is held in the closed state by the DHPR and goes to the semiopen state only during depolarization to generate unresolvable events. That list was not meant to be exhaustive and other possibilities might also exist. The data available at that time was insufficient to support any of the explanations more definitively.

The aims of this article are: 1), to confirm that the steady glows induced by Ry do not reflect calcium leaks caused by photo-damage but rather reflect Ca^{2+} fluxes through semiopen CRCs; and 2), to ascertain which one of the three possibilities offered in our preceding article most likely explains the mechanism underlying the nonsparking depolarization-evoked calcium transients. To achieve these goals, we employed a select group of Ry congeners, referred to herein as ryanoids, each of which is capable of inducing a semiopen state with a defined subconductance level that varies widely among the ryanoids. Correlations between the subconductance levels and the intensities of the steady glows the ryanoids generate might help establish whether the glows do in fact result from Ca^{2+} fluxes through CRCs that are in ryanoid-induced semiopen states. In addition, correlations between the intensities of the glows and those of the uniform calcium transients evoked by depolarization after the CRCs have been induced to a semiopen state by the ryanoids might provide information about the mechanism underlying the uniform depolarization-evoked calcium transients

In skeletal muscle, mutations of RyR1s cause the molecules to become leaky, resulting in malignant hyperthermia and central core disease. One attractive strategy to treat the diseases is to reduce the resting leak of the channels and yet preserve the ability of the channels to open on depolarization. Our results show that some ryanoids may have such ability and thus may lead to the development of therapeutic agents for treating the diseases.

METHODS

Composition of solutions

Relaxing solution (solution A): 120 mM K-glutamate, 1 mM $MgSO_4$, 0.1 mM K_2-EGTA, 5 mM K_2-PIPES, pH 7.0. Internal solution (solution B): 92.5 mM Cs-glutamate, 20 mM Na_2-creatine phosphate, 0.1 mM Cs_2-EGTA, 3 mM $MgCl_2$, 5 mM Na_2ATP, 5 mM glucose, 5 mM Cs-MOPS, 0.2 mM fluo-3, pH 7.0. The nominal free Ca^{2+} concentration was adjusted to 50 nM by adding $CaCl_2$. The nominal free Mg^{2+} concentration was estimated to be 0.13 mM following a method used by Fabiato (1988); see also Lacampagne et al. (1998). External solution (solution C): 117 mM TEA-CH_3SO_3, 5 mM Cs-MOPS, 2 mM $CaCl_2$, 1 μM tetrodotoxin, pH 7.1.

Fiber preparation

The experimental protocols followed those described previously (Hui et al., 2001). Experiments were performed on cut fibers from semitendinosus muscles of English frogs, *Rana temporaria*, cold-adapted in a refrigerator. In accordance with a procedure approved by the Institutional Animal Care and Use Committee, the animals were killed by decapitation and destruction of the brain and spinal cord. Cut fiber segments were dissected in solution A. A stretched fiber segment (sarcomere length 3.6–3.8 μm) was mounted in a double Vaseline-gap chamber designed for an inverted microscope (DiFranco et al., 1999). After saponin treatment (Irving et al., 1987) was applied to the fiber segments in the two end pools, the two pools were filled with solution B and the center pool with solution C. The membrane potential was clamped at $-$90 mV. About 40–50 min were allowed for fluo-3 to diffuse into the myoplasm before images were captured. All experiments were performed at room temperature (21–24°C).

Ryanoids

All ryanoids used in this study were synthesized and purified to $>$99.5%, using the methods described previously (Bidasee and Besch, 1998). Stock solution of each ryanoid was prepared by dissolving an appropriate amount of the ryanoid in solution C and applied to the center pool of the chamber. The effective concentration of each ryanoid from vesicle and bilayer studies was used initially as a guideline to determine the amount of ryanoid to be added to the center pool solution. Because the ryanoid molecules had to diffuse through connective tissues and the outer membranes of the fiber segment to reach the RyR targets, a concentration of 20-fold the K_d was applied in pilot experiments and then, if necessary, adjusted empirically such that the time course of its action on calcium sparks in cut fibers fell within the range of a few to $\sim$15 min.

Confocal imaging

The fluorescence (F) signal was monitored with a Nikon PCM2000 system consisting of a scan head mounted on a Nikon Diaphot 300 inverted microscope and an argon laser. The images were recorded in the line-scan mode using a Nikon Plan Apochromat 60$\times$ (1.2 n.a.) water immersion objective (Melville, NY). The image resolution was set at 1024 x-pixels $\times$ 1024 t-pixels. Each x-pixel covered 0.070 μm at a zoom factor of 3 and each t-pixel occupied 2.5 ms. Thus, all the images shown in this report have a full scale of 71.6 μm $\times$ 2.56 s, except for the cropped ones. The point-spread function of the microscope was estimated with 0.1 μm fluorescent

microspheres (Molecular Probes, Eugene, OR). The full-width half maximum values were ~0.3 μm in the x- and y-directions and ~0.6 μm in the z-direction. The scanning operation and data acquisition were executed with SimplePCI software (Compix, Tualatin, OR). Subsequent offline data analysis was performed with programs written in IDL (Research Systems, Boulder, CO).

Statistical tests of significance

The difference between the mean values of two sets of results was assessed with Student's two-tailed t-test. The difference was considered to be significant if $P < 0.05$.

RESULTS

Conversion of spontaneous calcium sparks to steady glows by ryanoids

To assess whether the steady glows observed in Ry-treated fibers (Hui et al., 2001) were indeed generated by fluxes of Ca^{2+} through semiopen CRCs, Ry was replaced by other ryanoids that exhibit larger or smaller subconductances. The rationale was that the intensity of the glow should be larger (or smaller) for a ryanoid that induces the CRC to a subconductance larger (or smaller) than that of Ry. At the time of the study, ryanodol (Ryol) was the only ryanoid known that induced a subconductance larger than that of Ry (see Table 1 in Discussion) and was used in the first series of experiments.

Fig. 1 shows the results from a resting fiber exposed to 1 mM Ryol. The line-scan image in the upper panel was recorded 4 min after the application of Ryol and was cropped to show only one triadic region bordered by two bright bands. The bright bands were confirmed in other fibers to coincide with the A-bands in bright-field images and agreed with the finding that fluo-3 molecules could be localized in the A-bands (Harkins et al., 1993). The F-ratio normalization procedure was not applied to the image because the $F(x,t)$ values at the location of the triad (indicated by the *arrow* on the left) was above the true $F_0(x)$ level most of the time. Normalization of all the pixels by the apparent $F_0(x)$ at that location would greatly reduce $\Delta F(x,t)/F_0(x)$ from their true values and thus obscure the glow. Instead, the F-intensity profile at the location of the triad was calculated (as shown below the image) to facilitate the visualization of the activities. Within a 2.5-s time frame, this trace captured an interesting array of events generated by 1 mM Ryol. The beginning of the trace shows active spark-like events that have longer time courses than the calcium sparks observed in other fibers (such as in Fig. 2 *A*). The event at ~300 ms was converted to a steady glow that lasted ~1 s. This glow was brighter than those generated by Ry, as reported in Hui et al. (2001). At ~1400 ms, the glow was terminated by a gap followed by a spark-like event at ~1500 ms, after which the trace displayed intense activities. However, it is difficult to determine whether these later activities were repetitive sparks or a glow with frequent gaps. This feature of reappearance of sparks was never observed in Ry-generated glows (Hui et al., 2001) and might reflect the reversible binding of Ryol to RyRs (Tinker et al., 1996; Tanna et al., 2000). The reappearance of sparks was observed in some other Ryol-treated fibers including the one shown in Fig. 2.

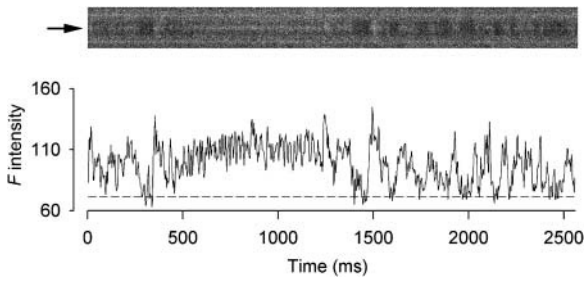

FIGURE 1 Effect of 1 mM Ryol on spontaneous calcium sparks. The upper part shows a line-scan image cropped to display the calcium events in a triadic region bordered by two bright bands. The F-intensity trace at the middle of the triadic region of the image is plotted below the image. Each point of the trace was obtained by averaging spatially the pixel (marked by the *arrow* on the left of the image) and its two neighboring pixels on each side. The sequence of activities includes calcium sparks followed by a steady glow, which reverts back to a spark followed by either high-frequency sparks or glow interrupted by frequent gaps. Sarcomere length 3.8 μm. The height of the cropped image is 5.9 μm.

The dashed line associated with the F-intensity profile in Fig. 1 represents the value of the background F_0 that was estimated by averaging the points in the troughs of the profile. The average value of $\Delta F/F_0$ during the glow was estimated to be 0.56. The peak $\Delta F/F_0$ value of the spark-like event immediately preceding the glow was estimated to be 0.93, which happened to be the same as the average of the peak values of the three brightest events in the trace. Thus, the ratio of glow/spark amplitudes for this occurrence was 0.60. This ratio doubles those we obtained from Ry-generated glows and is consistent with Ryol inducing a larger subconductance than Ry.

Some additional features of the action of 1 mM Ryol from another experiment are shown in Fig. 2, in which the effects of Ryol progressed at a pace different from that in Fig. 1. Each line-scan image in *A–D* was cropped to show four adjacent triadic regions (numbered *1–4*) separated by bright bands. Again, the F-ratio normalization procedure was not applied to the images for the reason explained above. The image in Fig. 2 *A* was scanned 1 min after the application of Ryol. The triad in region 3 showed very active calcium sparks with a frequency of 10 s^{-1}. Thus, reminiscent of the situation with Ry, the first effect of Ryol appears to be an increase in firing frequency of spontaneous calcium sparks. After another 1 min, the sparks in region 3 were converted to a steady glow and the sparking activities in region 2 were also enhanced (Fig. 2 *B*). In contrast to Fig. 1, the transition from sparks to glow in region 3 apparently occurred in the time interval between the two scans and was not captured.

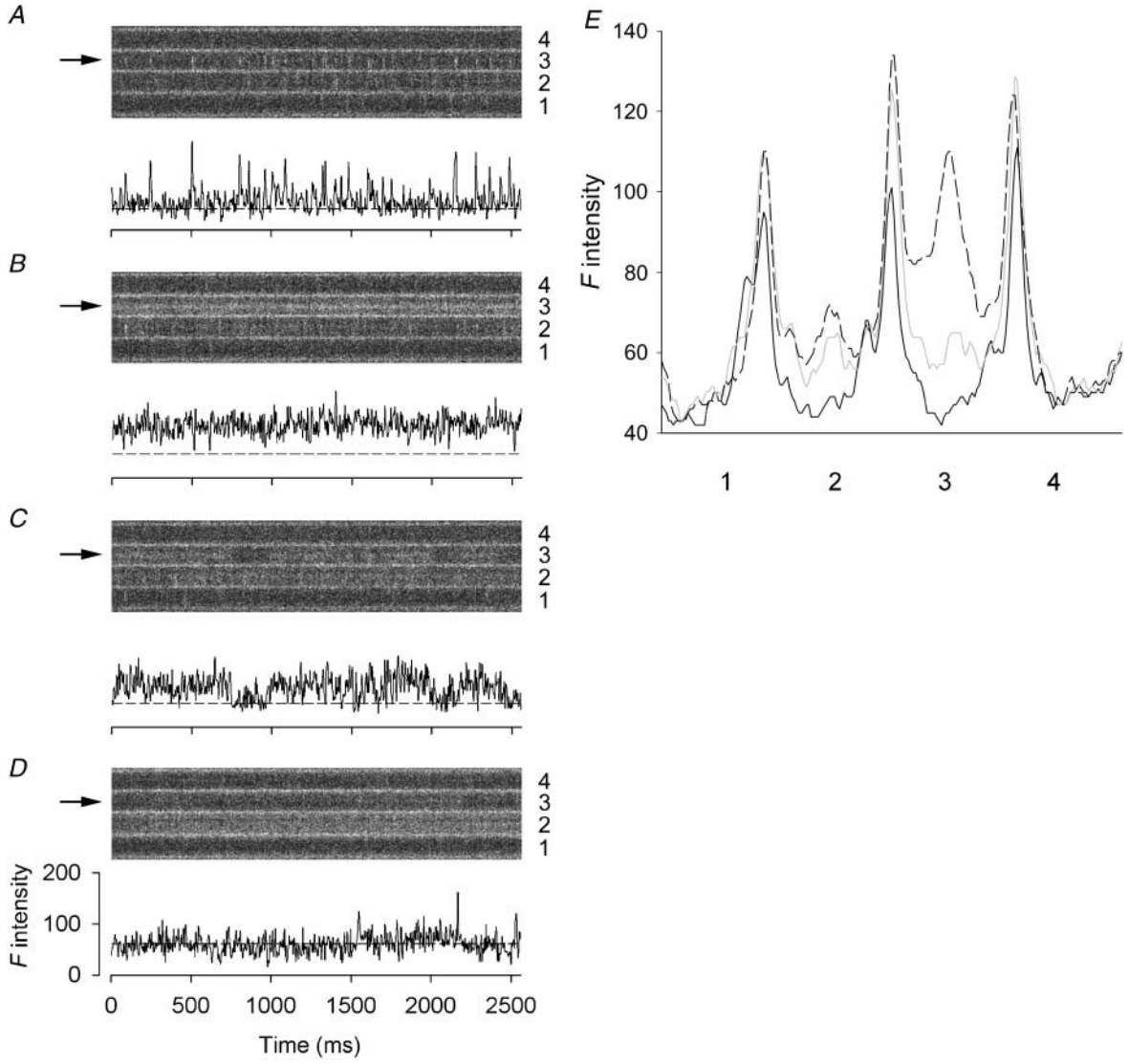

FIGURE 2 Effect of 1 mM Ryol on spontaneous calcium sparks. (*A–D*) The upper part of each panel shows a line-scan image cropped to display the calcium events in four neighboring triadic regions (marked by *1–4* on the right) separated by bright bands. The *F*-intensity trace at the middle of triadic region 3 of each image is plotted below the image. Each point of the trace was obtained by averaging spatially the pixel (marked by the arrow on the left of the image) and its two neighboring pixels on each side. The vertical and horizontal scales apply to all four traces. (*A*) High-frequency spontaneous sparks, (*B*) steady glow, (*C*) glow with gaps, (*D*) infrequent sparks, and (*E*) one-dimensional spatial *F* profiles. Each profile was obtained by averaging the values of the time pixels (horizontal direction) at each spatial location of a line-scan image and plotting the averaged values against the spatial locations (vertical direction). The triadic regions marked *1–4* in this panel correspond to the identically marked regions in *A–D*. The black curve was calculated from an image (not shown) scanned immediately after the application of Ryol; the shaded and dashed curves were calculated from the images shown in *A* and *B*, respectively. Sarcomere length 3.7 μm. The height of each cropped image is 16.1 μm.

The image in Fig. 2 *C* shows that the glow persisted after another 1 min, but was interrupted by some longer (200–250 ms) and briefer (≤100 ms) gaps. Such gaps were not apparent in the image of Fig. 1. Also, the glow in Fig. 2 *B* lasted the whole duration of 2.5 s and presumably continued for 1 min to Fig. 2 *C* or even longer, as compared to the 1-s duration in Fig. 1. In the next image taken after another 2 min (Fig. 2 *D*), the glow in region 3 had disappeared and a spark reappeared, consistent with reversible binding of Ryol to CRCs, while another glow appeared in region 2. It should be noted that, in all the images of Fig. 2, *A–D*, while the events were occurring in regions 2 and 3, the two neighboring regions 1 and 4 were inactive. To facilitate the visualization of the events in the images, the *F*-intensity traces at the locations marked by the arrows on the left are shown below each image, as was done in Fig. 1. The dashed line associated with each trace represents the background F_0 value that was estimated by a procedure described below.

Because of the intense activities in Fig. 2, *A–C*, the F_0 values in these three panels could not be estimated reliably

by the routine averaging procedure. Instead, they were estimated from another image that was recorded before any activity occurred, as illustrated in Fig. 2 *E*. Each of the three spatial *F*-intensity profiles in Fig. 2 *E* was obtained by compressing a cropped image in the horizontal direction into a one-dimensional plot. This was achieved by averaging all the *t*-pixels at each *x*-location and plotting the average values against the *x*-locations. The black profile was obtained from the image (not shown) that was scanned immediately after the application of Ryol and before any activity occurred in the triadic regions. The shaded and dashed profiles were obtained from the images shown in *A* and *B*, respectively. To account for the additional entry of fluo-3 from the end pools into the myoplasm as the experiment progressed, the black and shaded profiles were scaled appropriately such that their troughs in regions 1 and 4 match those of the dashed profile. The ''humps'' in regions 2 and 3 of the shaded profile above the black profile were due to the occurrences of calcium sparks whereas the huge elevation in region 3 of the dashed profile was caused by the occurrence of the steady glow. This scaling procedure provided a means to estimate the background F_0's for the shaded and dashed profiles when they could not be estimated by the routine averaging technique.

The dashed lines associated with the *F*-intensity traces in Fig. 2, *A–C*, represent the F_0 values adopted from the trough in region 3 of the black profile in Fig. 2 *E* after scaling the black profile individually for each of the other two profiles. That of Fig. 2 *D* was estimated by the routine averaging procedure. Based on the adopted F_0 value, the average value of $\Delta F/F_0$ during the glow in Fig. 2 *B* was estimated to be 1.39. The average of the peak $\Delta F/F_0$ values of the brightest sparks in Fig. 2 *A* was 2.16. Thus, the ratio of glow/spark amplitudes for these events was 0.64.

A total of 17 Ryol-generated glows were observed in 10 fibers. Averaged over all the glows, the ratio of glow/spark amplitudes was 0.55 ± 0.02 (mean ± SE). This value is shown in the left-most bin in the histogram of Fig. 4 *A*.

In some observations, a subsided glow could reappear in a later image, indicating a gap of long duration. This recovery of CRCs from the shut state to the semiopen state was never observed in Ry-treated fibers. It could be an indication of reversible binding of Ryol to the shutting sites on RyRs. Alternatively, because the SR does not contain infinite supply of Ca^{2+}, it is possible that the termination of a glow could be due to depletion of the SR content and reappearance of the glow could occur after the content is replenished. Nonetheless, because the amplitude of the glow in Fig. 2 was quite well maintained between panel *B* and panel *C*, it would take many minutes to deplete the SR content, at least in the triad studied in that fiber.

At the other end of the spectrum, if a ryanoid induces the CRCs to a subconductance level lower than that of Ry, then the intensity of the steady glow should be lower than that generated by Ry. To test this hypothesis, we used the semisynthetic ryanoid C_{10}-O_{eq} β-alanyl-ryanodol (βaRyol), which has been shown to modify skeletal CRCs to 14% of the full conductance state (Tripathy et al., 2000). βaRyol (0.2–1 mM) was applied to nine fibers and dim glows were detected in only two of them, probably because the glows in the others were too dim to be seen. One of the detectable glows is shown in Fig. 3. The cropped image in *A* was scanned 4 min after the application of 0.2 mM βaRyol. Some spontaneous sparks occurred toward the end of the 2.5-s interval. In the next cropped image (in *B*), a faint glow appeared at the same location.

Because the glow is very dim, we provide three methods to facilitate its visualization. First, the procedure used to generate Fig. 2 *E* was used again to compress the images in Fig. 3, *A* and *B*, to yield the black and red spatial *F* profiles, respectively, shown in Fig. 3 *C*. The black trace had been scaled to match the red trace. The small ''hump'' between the two bright bands in the black profile was due to the occurrences of the spontaneous calcium sparks. The larger ''hump'' in the red profile confirmed unequivocally the occurrence of the steady glow that was difficult to visualize in the raw image. Interestingly, this ''hump'' was much less prominent than that generated by Ryol in Fig. 2 *E*.

Secondly, the *F*-intensity traces at the locations marked by the arrows in Fig. 3, *A* and *B*, are displayed below each image. Because of the existence of the calcium sparks in the later segment of the image in Fig. 3 *A*, the black spatial *F* profile in Fig. 3 *C* did not provide an accurate estimate for the background F_0. To alleviate this problem, another spatial *F* profile was obtained by excluding the extreme right portion of the image that contained the sparks. The dashed line associated with the *F*-intensity trace in Fig. 3 *A* represents the value of F_0 obtained from this recalculated spatial *F* profile whereas that in Fig. 3 *B* represents the value of F_0 adopted from Fig. 3 *A* but after scaling. This adopted F_0 value lies below the trace, revealing the occurrence of the glow.

Thirdly, the image in Fig. 3 *B* was smoothed time-wise and scaled up eightfold in *F* intensity to enhance the appearance of the glow at the expense of saturating the pixels in the A-band regions. The processed image is shown in expanded spatial and temporal scales in Fig. 3 *D*. A color table is selected to facilitate the visualization of the glow. The color calibration bar at the bottom reveals that all pixels having *F*-intensity values >92 units are represented by white color irrespective of the exact values. The background is shown in black whereas the glow is a mixture of red and yellow.

The average value of $\Delta F/F_0$ during the glow in Fig. 3 *B* was estimated to be 0.28, which could be an underestimation of the true value if gaps occurred during the glow. Because the glow was so dim, we cannot identify gaps definitively. The average of the peak $\Delta F/F_0$ values of the brightest sparks in Fig. 3 *A* was 1.56. Thus, the ratio of glow/spark amplitudes for this set of records was 0.18. Averaged over a total of four βaRyol-generated glows, the ratio was 0.18 ± 0.02. This value is shown in the right-most bin in the histogram of Fig. 4 *A*.

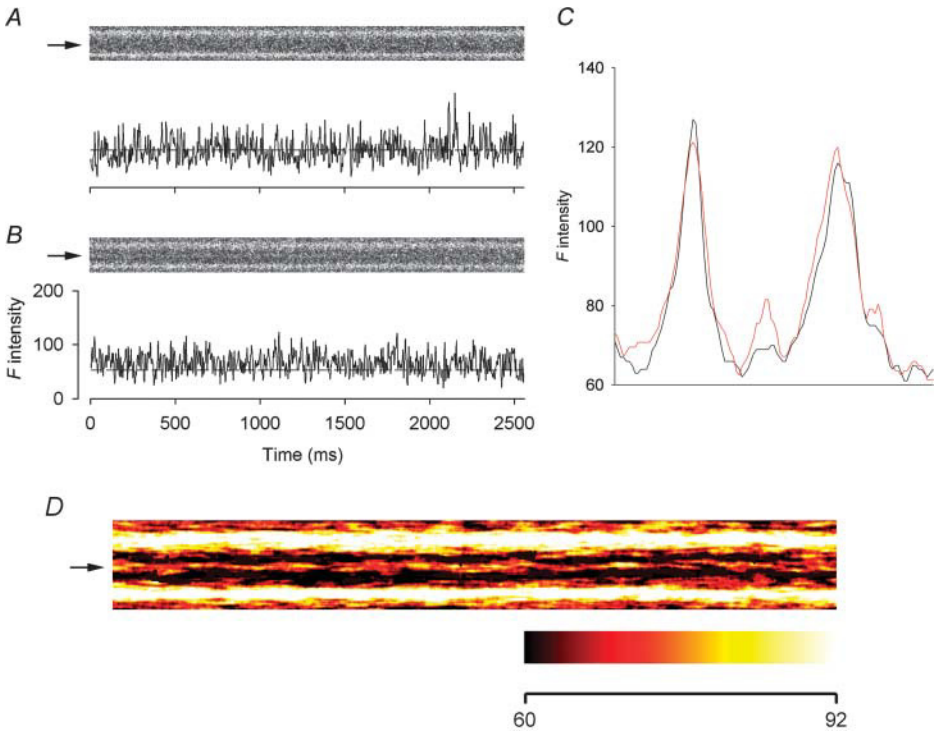

FIGURE 3 Effect of 0.2 mM βaRyol on spontaneous calcium sparks. (*A* and *B*) The upper part of each panel shows a line-scan image cropped to display the calcium events in a triadic region bordered by two bright bands. The *F*-intensity trace at the middle of the triadic region of each image is plotted below the image. Each point of the trace was obtained by averaging spatially the pixel (marked by the arrow on the left of the image) and its two neighboring pixels on each side. (*A*) Infrequent spontaneous sparks, (*B*) steady glow, and (*C*) one-dimensional spatial *F* profiles. The profiles were obtained by the procedure described in the legend of Fig. 2. The black and red curves were calculated from the images in *A* and *B*, respectively. The left end of each profile corresponds to the bottom edge of each image. (*D*) Expanded view of the image in *B*. Temporal smoothing was carried out by averaging each pixel time-wise with 15 pixels before and 15 pixels after it. A steady background *F* of 60 intensity units was subtracted from each pixel before the image was converted to pseudocolor. The color calibration bar at the bottom shows that the whole color scale covers 32 *F*-intensity units, a range equal to 1/8 of the full range of the raw data. Sarcomere length 3.8 μm. The height of each cropped image is 5.6 μm.

Because the glows generated by βaRyol were difficult to detect, experiments were performed next with another irreversible ryanoid, namely C_{10}-O_{eq} glycyl-ryanodine (gRy). In preliminary single-channel studies, we have determined that this ryanoid induces a subconductance of 0.16 ± 0.01 (n =3), which is slightly larger than that induced by βaRyol (see Table 1).

Experiments were performed on nine fibers with 20–40 μM gRy and 10 glows were observed in seven fibers (raw data not shown). Averaged over all the glows, the ratio of glow/spark amplitudes was 0.20 ± 0.10. This value is shown in the third bin from the left in the histogram of Fig. 4 *A*. Also, from Table 1 of our preceding article (Hui et al., 2001), the average ratio of glow/spark amplitudes for Ry-activated glows was 0.28 ± 0.02. This value is shown in the second bin from the left in the same histogram for comparison.

The results thus far show that, in cut skeletal muscle fibers, these ryanoids are capable of converting spontaneous sparks to steady glows of different intensities. The ratios of the glow/spark amplitudes follow the sequence:

$$\text{Ryol} > \text{Ry} > \text{gRy} > \beta\text{aRyol}. \quad (1)$$

The differences between the ratios of Ryol and Ry and between Ry and gRy are statistically significant, whereas that between gRy and βaRyol is insignificant. Because the order of these ratios parallels that of the subconductances induced by the ryanoids (see Table 1 in Discussion), the data supports the notion that the glows result from Ca^{2+} fluxes through CRCs in the semiopen state.

Suppression of depolarization-evoked calcium sparks and reduction of global calcium transients by ryanoids

We reported in our preceding article that, at concentrations of 1–2 μM, Ry was effective in suppressing depolarization-evoked calcium sparks, but transformed the calcium transient during depolarization to a uniform, nonsparking signal. In this article, we studied depolarization-evoked calcium sparks and transients after treatment with Ryol, gRy, or βaRyol. In the experiment shown in Fig. 5, the fiber was subjected to 500-ms depolarizing pulses to −75 mV (indicated by the *middle traces* in both panels). The image at the top of Fig. 5 *A* was recorded before the application of Ryol. It had been normalized by a *F*-ratio procedure, in which only the *t*-pixels before the onset of the pulse were used to calculate F_0 at each location, and had been converted to pseudocolor. A few faint spontaneous sparks occurred before depolarization. During depolarization, sparks were evoked very frequently. This is consistent with the findings in the preceding article (Fig. 7 of Hui et al., 2001).

The image at the top of Fig. 5 *B* was recorded 5 min after the application of 1 mM Ryol. It was the earliest

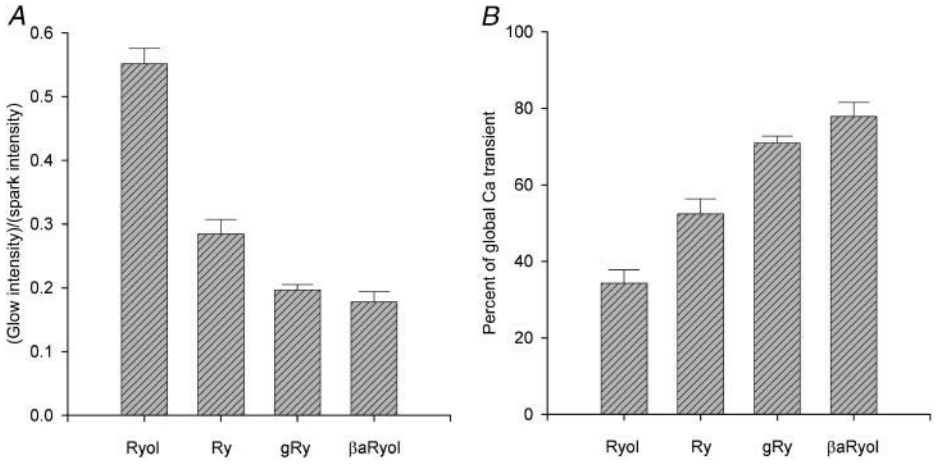

FIGURE 4 Effects of ryanoids on localized spontaneous and global depolarization-evoked calcium release. (*A*) Comparison of the normalized intensities of the steady calcium glows converted from spontaneous calcium sparks by different ryanoids. The intensity of each steady glow was divided by the intensity of the precursory spark to yield the ratio. [ryanoid] = 1 mM, 0.4–2 μM, 20–40 μM, 0.2–1 mM, and $n = 17, 14, 10, 4$ for Ryol, Ry, gRy, βaRyol, respectively. (*B*) Comparison of the residual depolarization-evoked global calcium transients affected by different ryanoids. Global calcium transients were elicited by 500-ms depolarizing pulses before and after the application of a ryanoid. Each value of $\Delta F_{500}/F_0$ in the presence of a ryanoid was divided by the control value to yield the percentage. [ryanoid] = 1 mM, 1–2 μM, 20–40 μM, 0.2–1 mM, and $n = 9, 9, 8, 5$ for Ryol, Ry, gRy, βaRyol, respectively. For the values in both panels, the differences between Ryol and Ry and between Ry and gRy are statistically significant, whereas that between gRy and βaRyol is insignificant. The error bars represent ± SE. For the selection of ryanoid concentrations, refer to the Methods section.

image showing complete abolition of spontaneous and depolarization-evoked calcium sparks. The absence of sparks was an indication of the induction of semiopen state in the active CRCs. As with Ry, the depolarizing pulse elicited a uniform calcium release that leads to a progressive increase in the *F* intensity throughout the depolarization period, but the increase was smaller than that observed with Ry (see Fig. 9 of Hui et al., 2001). One might wonder why no persistent glow can be visualized in Fig. 5 *B*. The reason for its absence is that any glow that existed would have been eliminated by the *F*-ratio procedure in the processed image shown in Fig. 5 *B*. Thus, the depolarization-activated increase in *F* intensity was contributed by additional calcium release on top of the steady calcium leak through semiopen CRCs. However, if the CRCs were ''locked'' rigidly in the semiopen state, they should not be able to open any further by a potential change in the outer membranes. Indeed, this *F* transient presented a surprise when we first discovered it

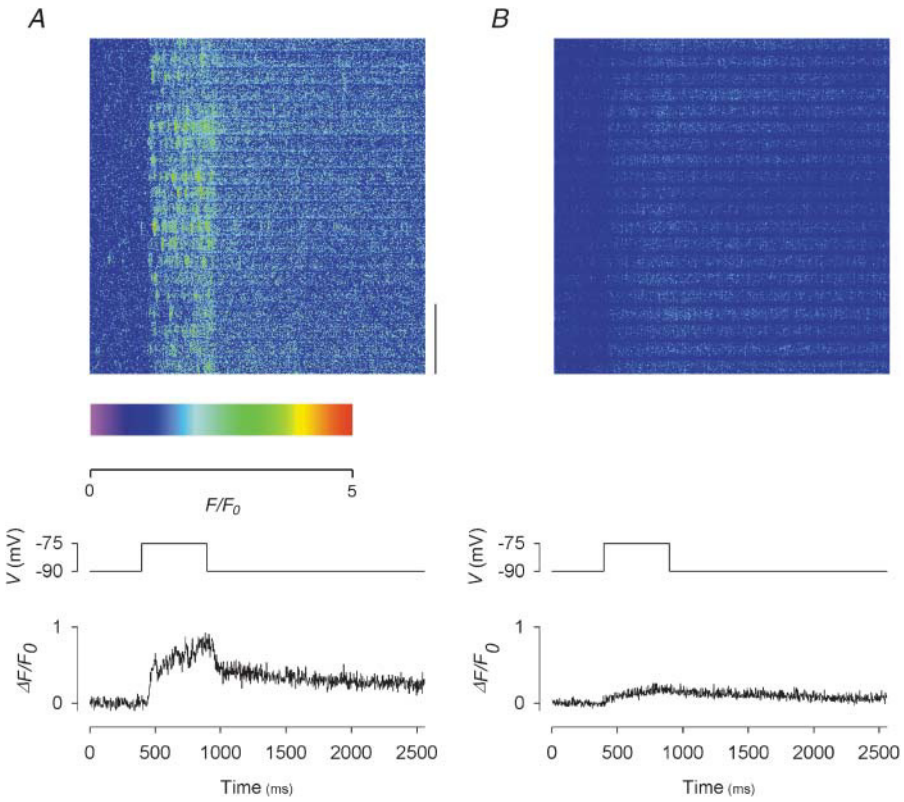

FIGURE 5 Effects of 1 mM Ryol on depolarization-evoked calcium sparks and global calcium transients. (*A*) Control before the application of Ryol; (*B*) in the presence of 1 mM Ryol. Each panel shows: (*top*) a line-scan image in pseudocolor; (*middle*) the depolarizing pulse used to trigger the calcium release; (*bottom*) the global $\Delta F(t)/F_0$ trace obtained by compressing the two-dimensional image vertically into a one-dimensional array. The vertical bar at the lower right corner of the image in *A* represents a length of 10 μm. The scale below the image in *A* indicates the color calibration. Sarcomere length 3.6 μm.

with Ry in our previous study. Although the F transient with Ryol is smaller than that with Ry, the new results reinforced our previous finding (see Discussion for possible explanations).

The bottom traces in Fig. 5, *A* and *B*, show the global $\Delta F(t)/F_0$ vs. t plots. Each point in a trace was obtained by averaging $\Delta F(x,t)/F_0(x)$ over the whole range of x in the image for a particular t, equivalent to compressing the two-dimensional image vertically to one dimension. Because the scan line spanned 71.6 μm, each point represents the signal averaged over ~20 sarcomeres. In the control trace (in *A*), $\Delta F(t)/F_0$ rose rapidly on depolarization to ~0.4 and then rose gradually through the end of the pulse. On repolarization, the decay also showed a fast and then a slow phase. By contrast, the test trace (in *B*) only rose slightly during depolarization. The value of $\Delta F/F_0$ at the end of the 500-ms depolarization will be referred to as $\Delta F_{500}/F_0$. It represents the amplitude of the calcium transient at that instant and was calculated by averaging the 181st–200th points after the onset of the pulse. Its value was 0.74 in the control trace and 0.19 in the test trace. The residual amplitude estimated from the ratio of test/control amplitudes was therefore 0.26. Furthermore, the presence of calcium sparks made the control trace in *A* much noisier, particularly during depolarization, than the test trace in *B*.

The same measurement was repeated in another fiber to which depolarizations were applied at four potentials (images and global $\Delta F(t)/F_0$ traces not shown). The values of $\Delta F_{500}/F_0$ from the control traces are plotted in Fig. 6 *A* as solid circles whereas those from the test traces in the presence of 1 mM Ryol are plotted as open circles. Control calcium release was not studied at −60 mV because of movement artifact and test calcium release was not recorded at −75 mV because the signal was too small. The residual amplitude estimated from the ratio of test/control amplitudes was 0.38 and 0.37 at −70 and −65 mV, respectively, with an average of 0.38 for this fiber.

Similar experiments were carried out in seven other fibers. Averaged over all the fibers, the residual amplitude in the presence of 1 mM Ryol is 0.34 ± 0.04, in the potential range between −75 and −65 mV. This value is shown in the leftmost bin in the histogram of Fig. 4 *B*.

The experiments shown in Figs. 5 and 6 *A* were also performed with the low subconductance ryanoids gRy and βaRyol. Fig. 7 *A* shows a control image at the top. Very faint spontaneous sparks occurred before depolarization and were barely detectable. During a 500-ms depolarization to −68 mV, sparks were evoked very frequently but not as bright as those in Fig. 5 *A*. In the later part of the depolarization, the frequency of the sparks was so high that the sparks could not be resolved individually. The image shown at the top of Fig. 7 *B* was recorded 19 min after the application of 20 μM gRy. Again, this was the earliest image showing complete abolition of spontaneous and depolarization-evoked calcium sparks. The same depolarization to −68 mV increased the F intensity uniformly, as with Ry and Ryol, but the increase was larger than with Ry.

The pair of traces shown at the bottom of Fig. 7 were obtained in the same way as those in Fig. 5. Again, the control trace in *A* was noisier than the test trace in *B*. In the control trace, the amplitude of the calcium transient was 1.06. Thus, although the depolarization-evoked sparks in Fig. 7 *A* were not as bright as those in Fig. 5 *A*, the higher frequency of occurrence of the sparks rendered the amplitude of the global calcium transient at −68 mV in this fiber larger than the counterpart (0.74) in Fig. 5 *A*. In the test trace, the amplitude of the global calcium transient was 0.81. Thus, the ratio of test/control amplitudes was 0.76 in this fiber. The same measurement was carried out in seven other fibers. Averaged over all the fibers, the residual amplitude in the

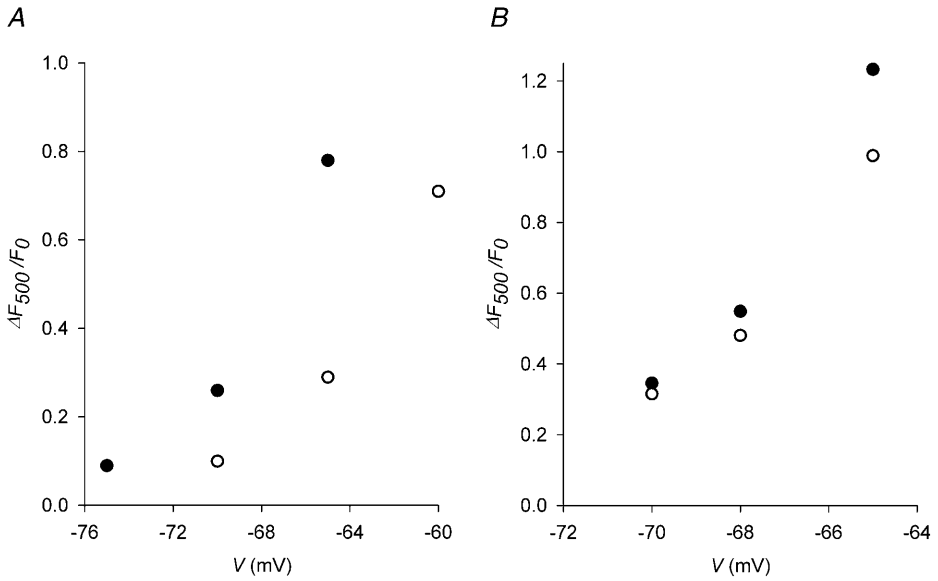

FIGURE 6 Effects of Ryol and βaRyol on global depolarization-evoked calcium transients. The global values of $\Delta F/F_0$ at the end of 500-ms depolarizing pulses (denoted by $\Delta F_{500}/F_0$) are estimated as described in the text and plotted against the potentials during the pulses. Solid circles represent the control values and open circles represent the test values. (*A*) Effect of 1 mM Ryol. Sarcomere length 3.7 μm. (*B*) Effect of 1 mM βaRyol. Sarcomere length 3.8 μm.

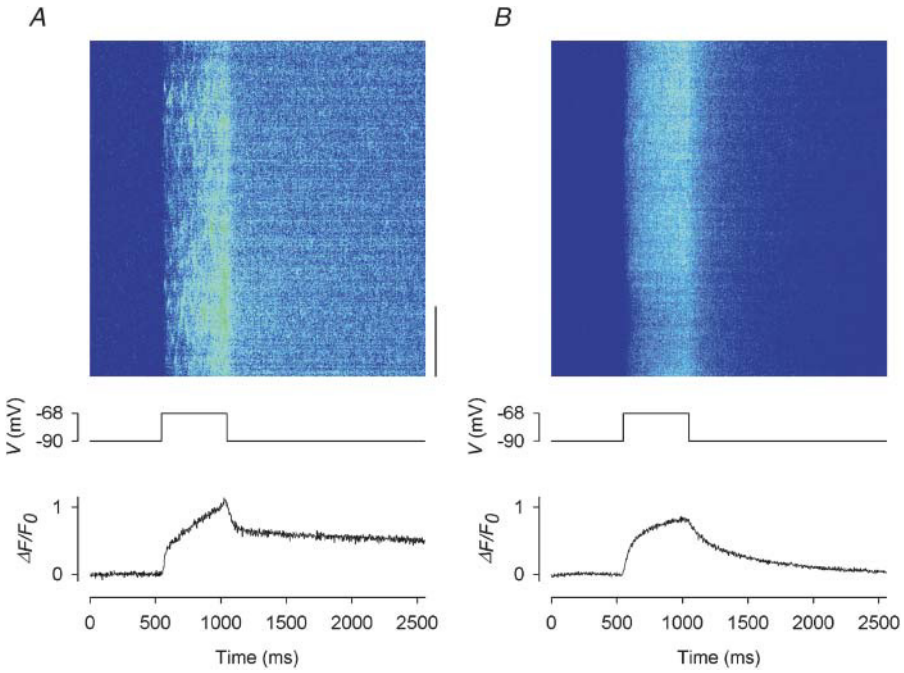

FIGURE 7 Effects of 20 μM gRy on depolarization-evoked calcium sparks and global calcium transients. (*A*) Control before the application of gRy; (*B*) in the presence of 20 μM gRy. Each panel shows: (*top*) a line-scan image in pseudocolor; (*middle*) the depolarizing pulse used to trigger the calcium release; (*bottom*) the global $\Delta F(t)/F_0$ trace obtained by compressing the two-dimensional image vertically into a one-dimensional array. The vertical bar at the lower right corner of the image in *A* represents a length of 10 μm. For color calibration, see the scale below the image in Fig. 5 *A*. Sarcomere length 3.7 μm.

presence of 20–40 μM gRy is 0.71 $\pm$ 0.02, in the potential range between -75 and -65 mV. This value is shown in the third bin from the left in the histogram of Fig. 4 *B*.

The experiment was repeated with 1 mM βaRyol on a fiber to which depolarizations were applied at three potentials (images and global $\Delta F(t)/F_0$ traces not shown). The values of $\Delta F_{500}/F_0$ from the control traces are plotted in Fig. 6 *B* as solid circles whereas those from the test traces are plotted as open circles. The average residual amplitude estimated from the ratios of test/control amplitudes was 0.86 between -70 and -65 mV.

The same measurement was made on four other fibers with 0.2–1 mM βaRyol. Averaged over all the fibers, the residual amplitude of the global calcium transient is 0.78 $\pm$ 0.04, in the potential range between -75 and -65 mV. This value is shown in the right-most bin in the histogram of Fig. 4 *B*. Also, from Table 2 of our preceding article, the average residual amplitude in the presence of 1–2 μM Ry was 0.52 $\pm$ 0.04. This value is shown in the second bin from the left in the same histogram for comparison.

The results show that Ryol, Ry, gRy, and βaRyol suppress depolarization-evoked calcium sparks but allow some residual calcium release in the form of a uniform, nonsparking transient. Fig. 4 *B* shows that the residual amplitudes of the global calcium transients are in an increasing order. The differences in residual amplitudes between Ryol and Ry and between Ry and gRy are statistically significant, whereas that between gRy and βaRyol is insignificant. Thus, it can be concluded that, after the CRCs have been induced to different subconductance states by various ryanoids, the residual amplitudes of the global calcium transient evoked by depolarization follow the sequence:

$$\text{Ryol} < \text{Ry} < \text{gRy} < \beta\text{aRyol}. \quad (2)$$

This sequence is in the reverse order of sequence 1.

In comparing sequences 1 and 2, it should be noted that sequence 1 describes a localized event at a single triad whereas sequence 2 describes an average of the events collected from triads in ~20 sarcomeres along the scan line, although both signals originate in peripheral myofibrils where the objective of the confocal microscope is focused. As such, nonuniformity well within the interior of the fiber due to voltage decrement along the T-tubules is of little concern. Nonetheless, there exists great variability of the calcium release signal among different triads. Results pertinent to sequence 1 were collected from more active triads whereas those pertinent to sequence 2 were averaged over active and not so active triads.

DISCUSSION

In this study, the effects of select ryanoids on localized spontaneous and depolarization-evoked calcium sparks and global calcium transients in cut skeletal muscle fibers were investigated. Like Ry, these ryanoids were capable of increasing the sparking frequency (Fig. 2 *A*), converting spontaneous sparks to steady glows lasting up to minutes (Figs. 1, 2, *B–D*, and 3 *B*) and, in the case of Ryol, generating gaps in glows (Fig. 2 *C*). Whether gaps existed in gRy- and βaRyol-generated glows is difficult to ascertain because the glows were very dim. Unlike Ry-generated glows, some Ryol-generated glows could subside and reappear (not shown) or be followed by sparks immediately (Fig. 1) or later (Fig. 2 *D*). The ratio of the intensity of the glow to that

of the precursory spark varied among the ryanoids and followed sequence 1. Furthermore, these ryanoids were able to suppress depolarization-evoked sparks effectively and transform the calcium release to uniform, nonsparking transients (Figs. 5 *B* and 7 *B*). The ratio of the amplitude of the global calcium transient in the presence of a ryanoid to that before followed sequence 2. The latter results suggest that CRCs that have been induced to a semiopen state by the select ryanoids are forbidden to generate calcium sparks during depolarization but can permit additional Ca^{2+} flux through them in response to the triggering signal from the voltage sensors.

Origin of the ryanoid-activated spontaneous events in cut fibers: comparison with electrical signals in single-channel recordings

The optical activities described in the preceding paragraph are reminiscent of the electrical events triggered by a ryanoid in single RyRs in bilayers. In the control state, a CRC makes brief transitions from the resting closed state to the full open state. When a low [ryanoid] is added to the *cis* side of the bilayer, the P_0, i.e., the frequency of the transitions from the closed to the full open state, of the CRC is increased (Bull et al., 1989; Pessah and Zimanyi, 1991). Second, the ryanoid induces the CRC to a subconductance (semiopen) state (Fleischer et al., 1985; Rousseau et al., 1987; Hymel et al., 1988; Buck et al., 1992; Tinker et al., 1996). Third, the semiopen CRC makes occasional transitions to the shut state (Zimanyi et al., 1992).

Fig. 8 *A* illustrates the optical signals observed when the released Ca^{2+} binds to fluo-3 in a muscle fiber. The opening of CRCs in a CRU generates a calcium spark. Thus, an increase in P_0 of the CRCs results in an increase in the frequency of sparks. Also, Ca^{2+} flux through semiopen CRCs is manifested as a steady glow. Furthermore, a temporary transition of the CRCs from the semiopen state to the shut state generates a gap in the glow. Fig. 8 *B* shows the optical signal generated by the event when the fiber is depolarized. It does not occur in the bilayer preparation. We hypothesize that when the CRCs are pulled open from the semiopen state to the full open state by the voltage sensors, a uniform elevation in F is generated (see next section).

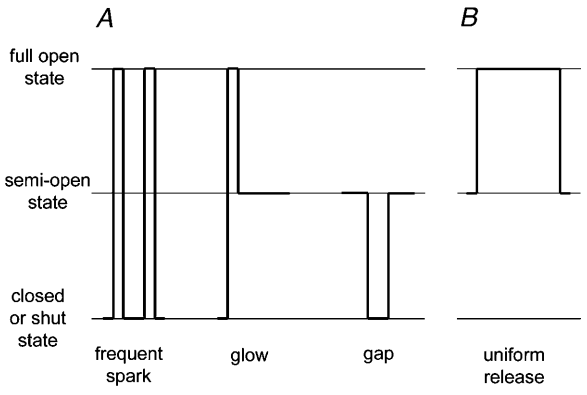

FIGURE 8 Schematic drawing showing correspondence between electrical events in single CRC recording and F signals in cut fibers affected by a low [ryanoid]. (*A*) (*Left*) Transitions of CRCs from resting state to full open state are manifested as calcium sparks. A ryanoid increases the open probability of such transitions, leading to more frequent sparks. (*Middle*) CRCs locked in a semiopen state generate a persistent glow. (*Right*) Occasional transitions of CRCs from the semiopen state to the shut state and back are manifested as gaps in the glow. (*B*) Transitions of CRCs from semiopen state to full open state as a result of the mechanical pull of DHPRs generate a uniform F transient (no counterpart in single-channel recording).

If the steady glow is indeed generated by Ca^{2+} flux through semiopen CRCs, the ratio of glow/spark amplitudes should be governed by, but not necessarily equal to (see below), the ratio of the subconductance to the full conductance of the CRCs. The ratios of glow/spark amplitudes from our experiments (represented by sequence 1) were shown in the histogram of Fig. 4 *A*. For comparison, the subconductances of skeletal and cardiac CRCs induced by the ryanoids, whichever available, are listed in the second and third columns of Table 1. Although the numerical values in the sequence of ratios of glow/spark amplitudes do not match exactly those in the sequences of subconductances, the overall trend of variation is conserved.

There are at least three explanations for the differences in values just mentioned. First, noise from various sources inevitably contributed to measurement errors. Second, the single-channel conductance of CRCs in muscle fibers might not be identical to that in bilayers, although at present, there is no direct evidence to support this possibility. Third, if calcium sparks and glows are not unitary events (i.e., not generated by single CRC) and if the numbers of CRCs involved in a spark and in a glow are different, then the ratios should be different from the subconductances. Early investigators hypothesized that spontaneous calcium sparks were unitary events (e.g., Cheng et al., 1993; Klein et al., 1996). More recent studies suggested that calcium sparks might not be unitary because of the discovery of smaller events (Lipp and Niggli, 1996; Parker et al., 1996; Shirokova and Rios, 1997; Shirokova et al., 1998) and investigators are leaning toward the possibility that a calcium spark might reflect the concerted opening of multiple CRCs. Morphological studies of the fine structures of triads showed that the proposed concerted

TABLE 1 Subconductances of RyR1 and RyR2 from bilayer studies

	Subconductance	
Ryanoid	RyR1	RyR2
Ryol	0.66*	0.69§
Ry	0.48†	0.57§
gRy	0.16‡	–
βaRyol	0.14*	–

*From Tripathy et al. (2000).
†From Buck et al. (1992).
‡K. Bidasee, L. Xu, G. Meissner and H. Besch, unpublished data.
§From Tinker et al. (1996).

opening of CRCs is feasible, as tens of CRCs group themselves into a cluster, which possibly serves as a CRU, in the SR (Franzini-Armstrong et al., 1999). Coupled gating of adjacent CRCs in the same CRU requires the accessory protein FKBP12 and was demonstrated by electrical recordings in bilayers by Marx et al. (1998, 2001). In some skeletal muscles, every other CRC in a CRU apposes a dihydropyridine receptor in the T-tubular membrane (Block et al., 1988). This led to the hypothesis that the CRCs that are linked to DHPRs are voltage gated and they initiate depolarization-evoked calcium sparks whereas the unlinked CRCs are calcium gated and they generate spontaneous calcium sparks (Klein et al., 1996; Shirokova and Rios, 1997).

From the amplitude of a calcium spark, the Ca^{2+} release flux through a CRU during the spark can be estimated (reviewed by Rios and Brum, 2002). On dividing the Ca^{2+} flux through the CRU by the unitary flux obtained from single-channel recordings, the number of active CRCs in the CRU can be calculated. This approach can be extended from the spark to the glow. Fig. 3 *B* of Cheng et al. (1993) showed that the glow amplitude was about half of the peak of the precursory spark. If a spark arises from the opening of a single CRC, then that ratio can be easily explained because the subconductance of a Ry-bound CRC is about half of the full conductance (Tinker et al., 1996). If a spark involves the opening of more than one CRC, then the CRCs must be tightly coupled in a way that they all undergo transitions to the subconductance state simultaneously. Thus, with respect to Ry action, cardiac CRCs appear to behave similarly in myocytes as in bilayers and probably a constant number of CRCs are involved in the conversion of a spark to glow.

In skeletal muscle, our previous study (Hui et al., 2001) showed that only dim sparks were converted to glows by Ry. Thus, perhaps a very small number of CRCs were involved in the sparks that were converted to glows. Also, the number of CRCs involved in a Ry-generated glow was probably half of that involved in the precursory spark. By comparison, Shtifman et al. (2000) estimated that the spark leading to an $IpTX_a$-generated glow involved at most four CRCs whereas Gonzalez et al. (2000) estimated the number to be at least six, although the glow might involve a single CRC. It remains to be determined whether the stoichiometry of channels in a spark to those in a glow varies from ryanoid to ryanoid. At present, because of the uncertainty in the single-channel current through frog skeletal CRCs, we are reluctant to estimate the absolute number of CRCs involved in a spark or a glow. As long as the numbers are different, it leaves plenty of leeway for the ratio of glow/spark amplitudes to differ from the subconductance for any ryanoid.

Origin of the depolarization-evoked uniform calcium release in the presence of a ryanoid

Our cut fiber studies showed that depolarization releases extra Ca^{2+} steadily (Figs. 5 *B* and 7 *B*; see also Fig. 9 *B* of Hui et al., 2001), in addition to the voltage-independent flux through semiopen CRCs. This implies that the gates of the CRCs might not be ''locked'' rigidly in the semiopen conformation. In our preceding article in which the effects of Ry were reported, we offered three possibilities (see Introduction) to explain this unexpected finding. Results from this study with the select ryanoids provide further insights to help us evaluate which of the three proposed possibilities best explains the underlying mechanism. A key piece of information that emerges from the results is the inverse relationship between sequences 1 and 2, i.e., an inverse relationship between the relative amplitudes of the spontaneous glows and the residual amplitudes of the depolarization-evoked calcium transients.

A varying degree of SR Ca^{2+} depletion might contribute slightly to the trend in sequence 2, but probably all of it. The reason is that the image used in each experiment to estimate the residual amplitude in sequence 2 was always recorded early on before significant depletion of SR Ca^{2+} occurred. It was always the earliest image that showed complete abolition of depolarization-evoked calcium sparks. Also, application of a larger depolarizing pulse later in the experiment always elicited a large calcium transient and prominent movement artifact, indicating that the signal used in the data analysis was not limited by the amount of releasable Ca^{2+}.

If the inverse relationship between sequences 1 and 2 is not totally caused by depletion of SR Ca^{2+}, it could be explained alternatively by one of the three possibilities mentioned in the Introduction section. If the glow and the nonsparking depolarization-evoked release are generated by two separate populations of CRCs, there is no a priori reason to expect the signals from the two populations to have an inverse relationship. Thus, possibility b is considered less likely. Possibility c is also unlikely because, if unlinked CRCs undergo transitions from the closed to the semiopen state to generate a spontaneous glow and linked CRCs make the same transitions on depolarization to generate the uniform *F* transient, then the two signals should be proportionally related instead of inversely related and so is inconsistent with the relationship between the two sequences. For possibility a, on the other hand, depolarization triggers a transition of the ryanoid-bound CRCs from the semiopen state to the full open state to generate a uniform *F* transient. Suppose semiopen state 2 induced by ryanoid 2 is at a higher level than semiopen state 1 induced by ryanoid 1. Although glow 2 has a larger amplitude than glow 1, there is less leeway for the CRCs to make transitions from semiopen state 2 to the full open state than from semiopen state 1, leading to a smaller uniform *F* transient 2 than uniform *F* transient 1. This is consistent with the inverse relationship between sequences 1 and 2. This piece of information is only available through studies in muscle fibers but not in the bilayer preparation.

Can CRCs serve as a therapeutic target to regulate intracellular free Ca^{2+}?

The inverse relationship between sequences 1 and 2 agrees with the idea that, when a ryanoid acts on CRCs, the gates are moved to a semiopen position but are not rigidly locked. On depolarization, the gates can be opened further and allow additional Ca^{2+} to be released from the SR. It also implies that the smaller the subconductance induced by the ryanoid, the greater the amount of Ca^{2+} released during depolarization. These findings may provide a therapeutic strategy for treating ''leaky CRC'' diseases, such as malignant hyperthermia and central core disease (Avila and Dirksen, 2001). However, to be useful as such a pharmacological agent, a ryanoid needs to be RyR1 isoform specific, having extremely low subconductance capability, specific for the semiopen state binding site and reversible.

We acknowledge the Biomedical Confocal Systems Division of Nikon Inc. for technical support on the PCM2000 hardware and Compix Inc. for technical support on the SimplePCI software.

This project was supported by grants from the National Institutes of Health (NS21955 to C.S.H. and HL66898 to K.R.B.) and a grant from the Showalter Trust to H.R.B., Jr.

REFERENCES

Avila, G., and R. T. Dirksen. 2001. Functional effects of central core disease mutations in the cytoplasmic region of the skeletal muscle ryanodine receptor. *J. Gen. Physiol.* 118:277–290.

Bidasee, K. R., and H. R. Besch, Jr. 1998. Structure function relationships among ryanodine derivatives. *J. Biol. Chem.* 273:12176–12186.

Bidasee, K. R., L. Xu, G. Meissner, and H. R. Besch, Jr. 2003. Diketo pyridyl ryanodine has three concentration-dependent effects on the cardiac calcium release channel/ryanodine receptor. *J. Biol. Chem.* 278:14237–14248.

Block, B. A., T. Imagawa, K. P. Campbell, and C. Franzini-Armstrong. 1988. Structural evidence for direct interaction between the molecular components of the transverse tubule/sarcoplasmic reticulum junction in skeletal muscle. *J. Cell Biol.* 107:2587–2600.

Buck, E., I. Zimanyi, J. J. Abramson, and N. Pessah. 1992. Ryanodine stabilizes multiple conformational states of the skeletal muscle calcium release channel. *J. Biol. Chem.* 267:23560–23567.

Bull, R., J. J. Marengo, B. A. Suarez-Isla, P. Donoso, J. L. Sutko, and C. Hidalgo. 1989. Activation of calcium channels in sarcoplasmic reticulum from frog muscle by nanomolar concentrations of ryanodine. *Biophys. J.* 56:749–756.

Cheng, H., W. J. Lederer, and M. B. Cannell. 1993. Calcium sparks: elementary events underlying excitation-contraction coupling in heart muscle. *Science.* 262:740–744.

DiFranco, M., M. Quinonez, D. A. DiGregorio, A. M. Kim, R. Pacheco, and J. L. Vergara. 1999. Inverted double-gap isolation chamber for high-resolution calcium fluorimetry in skeletal muscle fibers. *Pflugers Arch.* 438:412–418.

Fabiato, A. 1988. Computer programs for calculating total from specified free or free from specified total ionic concentrations in aqueous solutions containing multiple metals and ligands. *Methods Enzymol.* 157:378–417.

Fleischer, S., E. M. Ogunbunmi, M. C. Dixon, and E. A. M. Fleer. 1985. Localization of Ca^{++} release channels with ryanodine in junctional terminal cisternae of sarcoplasmic reticulum of fast skeletal muscle. *Proc. Natl. Acad. Sci. USA.* 82:7256–7259.

Franzini-Armstrong, C., F. Protasi, and V. Ramesh. 1999. Shape, size, and distribution of Ca^{2+} release units and couplons in skeletal and cardiac muscles. *Biophys. J.* 77:1528–1539.

Gonzalez, A., W. G. Kirsch, N. Shirokova, G. Pizarro, G. Brum, I. N. Pessah, M. D. Stern, H. Cheng, and E. Rios. 2000. Involvement of multiple intracellular release channels in calcium sparks of skeletal muscle. *Proc. Natl. Acad. Sci. USA.* 97:4380–4385.

Harkins, A. B., N. Kurebayashi, and S. M. Baylor. 1993. Resting myoplasmic free calcium in frog skeletal muscle fibers estimated with fluo-3. *Biophys. J.* 65:865–881.

Hui, C. S., K. R. Bidasee, and H. R. Besch, Jr. 2001. Effects of ryanodine on calcium sparks in cut twitch fibres. *J. Physiol. (Lond.).* 534:327–342.

Hymel, L., M. Inui, S. Fleischer, and H. Schindler. 1988. Purified ryanodine receptor of skeletal muscle sarcoplasmic reticulum forms Ca^{++}-activated oligomeric Ca^{++} channels in planar bilayers. *Proc. Natl. Acad. Sci. USA.* 85:441–445.

Irving, M., J. Maylie, N. L. Sizto, and W. K. Chandler. 1987. Intrinsic optical and passive electrical properties of cut frog twitch fibers. *J. Gen. Physiol.* 89:1–40.

Jenden, D. J., and A. S. Fairhurst. 1969. The pharmacology of ryanodine. *Pharmacol. Rev.* 21:1–25.

Klein, M. G., H. Cheng, L. F. Santana, Y.-H. Jiang, W. J. Lederer, and M. F. Schneider. 1996. Two mechanisms of quantized calcium release in skeletal muscle. *Nature.* 379:455–458.

Lacampagne, A., M. G. Klein, and M. F. Schneider. 1998. Modulation of the frequency of spontaneous sarcoplasmic reticulum Ca^{2+} release events (Ca^{2+} sparks) by myoplasmic [Mg^{2+}] in frog skeletal muscle. *J. Gen. Physiol.* 111:207–224.

Lipp, P., and E. Niggli. 1996. Submicroscopic calcium signals as fundamental events of excitation-contraction coupling in guinea-pig cardiac myocytes. *J. Physiol. (Lond.).* 492:31–38.

Lopez-Lopez, J. R., P. S. Shacklock, C. W. Balke, and W. G. Wier. 1994. Local, stochastic release of Ca^{2+} in voltage-clamped rat heart cells: visualization with confocal microscopy. *J. Physiol. (Lond.).* 480:21–29.

Marx, S. O., J. Gaburjakova, M. Gaburjakova, C. Henrikson, K. Ondrias, and A. R. Marks. 2001. Coupled gating between cardiac calcium release channels (ryanodine receptors). *Circ. Res.* 88:1151–1158.

Marx, S. O., K. Ondrias, and A. R. Marks. 1998. Coupled gating between individual skeletal muscle Ca^{2+} release channels (ryanodine receptors). *Science.* 281:818–821.

Parker, I., W. J. Zang, and W. G. Wier. 1996. Ca^{2+} sparks involving multiple Ca^{2+} release sites along Z-lines in rat heart cells. *J. Physiol. (Lond.).* 497:31–38.

Pessah, I. N., and I. Zimanyi. 1991. Characterization of multiple [^{3}H]ryanodine binding sites on the Ca^{2+} release channel of sarcoplasmic reticulum from skeletal and cardiac muscle: evidence for a sequential mechanism in ryanodine action. *Mol. Pharmacol.* 39:679–689.

Rios, E., and G. Brum. 2002. Ca^{2+} release flux underlying Ca^{2+} transients and Ca^{2+} sparks in skeletal muscle. *Front. Biosci.* 7:d1195–d1211.

Rousseau, E., J. S. Smith, and G. Meissner. 1987. Ryanodine modifies conductance and gating behavior of single Ca^{2+} release channel. *Am. J. Physiol.* 253:C364–C368.

Shirokova, N., J. Garcia, and E. Rios. 1998. Local calcium release in mammalian skeletal muscle. *J. Physiol. (Lond.).* 512:377–384.

Shirokova, N., and E. Rios. 1997. Small event Ca^{2+} release: a probable precursor of Ca^{2+} sparks in frog skeletal muscle. *J. Physiol. (Lond.).* 502:3–11.

Shtifman, A., C. W. Ward, J. Wang, H. H. Valdivia, and M. F. Schneider. 2000. Effects of Imperatoxin A on local sarcoplasmic reticulum Ca^{2+} release in frog skeletal muscle. *Biophys. J.* 79:814–827.

Tanna, B., W. Welch, L. Ruest, J. L. Sutko, and A. J. Williams. 2000. The interaction of a neutral ryanoid with the ryanodine receptor channel provides insights into the mechanisms by which ryanoid binding is modulated by voltage. *J. Gen. Physiol.* 116:1–9.

Tinker, A., J. L. Sutko, L. Ruest, P. Deslongchamps, W. Welch, J. A. Airey, K. Gerzon, K. R. Bidasee, H. R. Besch, Jr., and A. J. Williams.

1996. Electrophysiological effects of ryanodine derivatives on the sheep cardiac sarcoplasmic reticulum calcium-release channel. *Biophys. J.* 70: 2110–2119.

Tripathy, A., K. R. Bidasee, G. Meissner, and H. R. Besch, Jr. 2000. Ryanodine derivatives, ryanodol and β-alanyl ryanodol induce reversible, voltage-dependent substate behavior in skeletal muscle sarcoplasmic reticulum Ca^{2+} release channels (CRCs). *Biophys. J.* 78: 425a. (Abstr.)

Tsugorka, A., E. Rios, and L. A. Blatter. 1995. Imaging elementary events of calcium release in skeletal muscle cells. *Science*. 269:1723–1726.

Zimanyi, I., E. Buck, J. J. Abramson, M. M. Mack, and I. N. Pessah. 1992. Ryanodine induces persistent inactivation of the Ca^{2+} release channel from skeletal muscle sarcoplasmic reticulum. *Mol. Pharmacol*. 42:1049–1057.